Neuron
Article

Neuroligin 2 Drives Postsynaptic Assembly at Perisomatic Inhibitory Synapses through Gephyrin and Collybistin

Alexandros Poulopoulos,[1,7] Gayane Aramuni,[2,7] Guido Meyer,[1] Tolga Soykan,[1] Mrinalini Hoon,[1] Theofilos Papadopoulos,[4] Mingyue Zhang,[2] Ingo Paarmann,[4] Céline Fuchs,[5] Kirsten Harvey,[5] Peter Jedlicka,[6] Stephan W. Schwarzacher,[6] Heinrich Betz,[4] Robert J. Harvey,[5] Nils Brose,[1,3] Weiqi Zhang,[2,3,8,9,*] and Frédérique Varoqueaux[1,3,8,*]

[1]Department of Molecular Neurobiology, Max Planck Institute of Experimental Medicine, Göttingen, Germany
[2]Center for Physiology and Pathophysiology, Georg August University, Göttingen, Germany
[3]DFG Center for the Molecular Physiology of the Brain, Göttingen, Germany
[4]Department of Neurochemistry, Max Planck Institute of Brain Research, Frankfurt/Main, Germany
[5]Department of Pharmacology, The School of Pharmacy, London, UK
[6]Department of Clinical Neuroanatomy, Goethe University, Frankfurt/Main, Germany
[7]These authors contributed equally to this work
[8]These authors contributed equally to this work
[9]Present address: Laboratory of Molecular Psychiatry, Department of Psychiatry, Westfälische Wilhelms University, Münster, Germany
*Correspondence: wzhang@uni-muenster.de (W.Z.), varoqueaux@em.mpg.de (F.V.)
DOI 10.1016/j.neuron.2009.08.023

SUMMARY

In the mammalian CNS, each neuron typically receives thousands of synaptic inputs from diverse classes of neurons. Synaptic transmission to the postsynaptic neuron relies on localized and transmitter-specific differentiation of the plasma membrane with postsynaptic receptor, scaffolding, and adhesion proteins accumulating in precise apposition to presynaptic sites of transmitter release. We identified protein interactions of the synaptic adhesion molecule neuroligin 2 that drive postsynaptic differentiation at inhibitory synapses. Neuroligin 2 binds the scaffolding protein gephyrin through a conserved cytoplasmic motif and functions as a specific activator of collybistin, thus guiding membrane tethering of the inhibitory postsynaptic scaffold. Complexes of neuroligin 2, gephyrin and collybistin are sufficient for cell-autonomous clustering of inhibitory neurotransmitter receptors. Deletion of neuroligin 2 in mice perturbs GABAergic and glycinergic synaptic transmission and leads to a loss of postsynaptic specializations specifically at perisomatic inhibitory synapses.

INTRODUCTION

Accurate and balanced synaptic transmission is essential for the function of neuronal circuits. The coupling of transmitter release with transmitter-specific receptors is tightly coordinated between presynaptic and postsynaptic neurons. In precise apposition to sites of presynaptic terminal contact, the neuronal plasma membrane undergoes postsynaptic differentiation, leading to the accumulation of scaffolds and receptors. Cell adhesion molecules have a pivotal role in this process (Yamagata et al., 2003), but the mechanisms that determine synapse- and transmitter-specific protein recruitment events remain largely unknown.

The transsynaptic cell adhesion system formed by presynaptic neurexins (NX; Ullrich et al., 1995; Ushkaryov et al., 1992, 1994) and postsynaptic neuroligins (NL1-4; Ichtchenko et al., 1995, 1996; Jamain et al., 2008) is of particular importance for the assembly of synaptic specializations (Chih et al., 2005; Varoqueaux et al., 2006; Craig and Kang, 2007). At excitatory glutamatergic synapses, the molecular organization of postsynaptic glutamate receptors relies on a network of PDZ-domain-mediated protein interactions (Kim and Sheng, 2004). NLs interact with scaffolding proteins such as PSD95 and S-SCAM (Hirao et al., 1998; Irie et al., 1997; Meyer et al., 2004) through a conserved cytoplasmic PDZ-binding motif. The most prominent NL to specifically function at excitatory synapses is NL1. It is typically present at glutamatergic postsynapses (Song et al., 1999), and its deletion causes specific deficits in excitatory but not inhibitory transmission in the forebrain (Chubykin et al., 2007).

The NX-NL cell adhesion system is also of critical importance at inhibitory synapses, although the corresponding NX (Kang et al., 2008) and NL (Chih et al., 2006; Graf et al., 2004; Varoqueaux et al., 2004) isoforms are distinct from those at excitatory synapses. Most notably, NL2 is the only adhesion protein known to be constitutively and selectively present at inhibitory postsynaptic specializations (Varoqueaux et al., 2004). NL2 is involved in the differentiation and maturation events at nascent inhibitory postsynapses, as indicated by the observation that exogenous surface clustering of NL2 in cultured neurons induces the recruitment of the inhibitory synapse-specific postsynaptic scaffolding protein gephyrin to cluster sites (Graf et al., 2004). Gephyrin is a central component of both glycinergic and GABAergic postsynapses (Prior et al., 1992; Moss and Smart, 2001) and is critical

for the postsynaptic localization of both glycine (Kirsch et al., 1993; Feng et al., 1998) and $GABA_A$ receptors (Essrich et al., 1998; Kneussel et al., 1999). Gephyrin forms a hexagonal scaffold that directly binds glycine receptors (Meyer et al., 1995) and potentially also $GABA_A$ receptors (Tretter et al., 2008). Thus, postsynaptic targeting of gephyrin is central to inhibitory postsynaptic differentiation. However, the mechanisms underlying its specific localization at sites of inhibitory axon terminal contact have remained enigmatic.

A key protein implicated in the recruitment of gephyrin to developing postsynaptic sites is collybistin (Kins et al., 2000). Collybistin is able to attach gephyrin to the membrane by binding both gephyrin and membrane lipids (Harvey et al., 2004; Kalscheuer et al., 2009; Kins et al., 2000). Indeed, a truncated collybistin isoform translocates gephyrin from large cytoplasmic aggregates to the plasma membrane of nonneuronal cells (Harvey et al., 2004; Kins et al., 2000). Mouse genetic evidence also indicates a role of collybistin in postsynaptic differentiation as collybistin deletion results in a striking loss of gephyrin and $GABA_A$ receptor clusters in the hippocampus (Papadopoulos et al., 2007, 2008). The underlying mechanisms of collybistin function, however, remain unclear since only full-length isoforms, which do not show gephyrin-targeting activity, are expressed endogenously (Kins et al., 2000; Papadopoulos et al., 2007).

In the present study, we identified interactions of NL2 with the key components of the inhibitory postsynaptic scaffold: gephyrin and collybistin. We found that complex formation between these proteins activates collybistin-driven gephyrin tethering to the plasma membrane and is sufficient for the reconstitution of self-organizing "postsynaptic" elements containing clustered NL2, gephyrin, collybistin, and $GABA_A$ receptors in nonneuronal cells. Furthermore, we obtained in vivo evidence for the involvement of NL2 in the specific synaptic recruitment of $GABA_A$ and glycine receptors and identified perisomatic synapses as the major sites of NL2 function. Based on our findings, we propose a molecular model according to which NL2 functions as an organizer of inhibitory postsynaptic differentiation.

RESULTS

NLs Bind Gephyrin through a Conserved Cytoplasmic Motif

To identify novel cytoplasmic interaction partners of NL2, we performed a yeast-two-hybrid (YTH) screen of a rat brain cDNA library using the NL2 cytoplasmic domain ($NL2_{CD}$) lacking the three C-terminal residues as bait (Figure 1A). This construct is unable to interact with PDZ domain proteins, which have dominated previous YTH screens (Irie et al., 1997; Meyer et al., 2004). Over 500 prey clones derived from the screen were sequenced, leading to the identification of 30 candidate interaction partners of NL2 (Table S1). Among these were two independent gephyrin preys, one full-length clone corresponding to the gephyrin P1 splice variant and one C-terminal fragment (residues 286–768), which encompasses the gephyrin E domain.

YTH assays with the full-length cytoplasmic domains of the rodent NL paralogs showed that all four NLs can interact with gephyrin (Figure 1B). Using site-directed mutagenesis of selected residues, we identified a conserved tyrosine in the NL cytoplasmic domains (designated by a dot in Figure 1A) that is required for gephyrin binding in yeast. Substitution of this residue with alanine in NL1 (Y782A) or NL2 (Y770A) abolished the interaction with gephyrin but did not affect binding to PDZ domains (Figure 1C).

The interaction of NL2 with gephyrin was further examined using a chemical crosslinking approach that had previously been employed to identify postsynaptic protein complexes (Leonard et al., 1998). Native NL2-gephyrin complexes were detected in mouse brain homogenates after crosslinking, SDS extraction, and immunoprecipitation (IP) of endogenous NL2. Gephyrin was not detected in corresponding control precipitates from NL2 knock-out ($NL2^{-/-}$) mice (Figure 1D). Complexes of tagged HA-NL2 with GFP-gephyrin were similarly detected after in situ crosslinking in transfected nonneuronal cells, indicating that no additional neuron-specific factors are required for interaction. Consistent with our observations in yeast, the HA-NL2/Y770A mutant was not crosslinked with gephyrin in transfected cells (Figure 1E). Finally, soluble NL2-gephyrin complexes were detected in vitro as recombinant GST-$NL2_{CD}$-bound His-tagged E domain gephyrin (residues 316–736), while the corresponding NL2/Y770A mutant did not (Figure 1F).

Tyrosine 770 of NL2, critical for gephyrin binding, belongs to a 15 residue stretch that is highly conserved in all four NLs (framed in Figure 1A). This sequence was inserted into the cytoplasmic domain of the unrelated transmembrane protein HA-CD8α to yield the chimera HA-CD8α/GB (Figure 1G). Using the in situ crosslinking approach in transfected cell-lines, we observed that HA-CD8α/GB interacted with GFP-gephyrin, as did HA-NL2 but not HA-CD8α (Figure 1H). As these 15 residues are sufficient to mediate gephyrin binding and are conserved in all NLs, we propose that they represent a novel gephyrin-binding (GB) motif characteristic to the NL protein family.

The GB Motif Contributes to the Recruitment of Gephyrin to NL2 Clusters in Neurons

Gephyrin was previously found to be recruited at sites where NL2 is clustered on the plasma membrane of cultured neurons (Graf et al., 2004). To examine whether the direct interaction that we identified between NL2 and gephyrin is involved in this process, we established a quantifiable recruitment assay in hippocampal cultures. Rat neurons were transfected with extracellularly HA-tagged proteins and treated with anti-HA and anti-isotypic antibodies prior to fixation. This treatment induced the acute clustering of HA-NL2 at extrasynaptic sites on the neuronal surface and the recruitment of endogenous gephyrin to these clusters (Figure S1).

The ability of wild-type NL2, NL2 mutants, and chimeras to recruit gephyrin to extrasynaptic HA clusters was quantified in neurons from $NL2^{-/-}$ mice to avoid the possibility of transfected NL2 mutants oligomerizing with endogenous NL2 (Comoletti et al., 2006). While gephyrin coclustering was generally less robust in this system, potentially as a direct result of the genotype (see below), significant differences between the proteins examined were observed. The gephyrin-binding-deficient mutant HA-NL2/Y770A recruited endogenous gephyrin significantly less robustly than nonmutated HA-NL2. Additionally, the HA-CD8α/GB

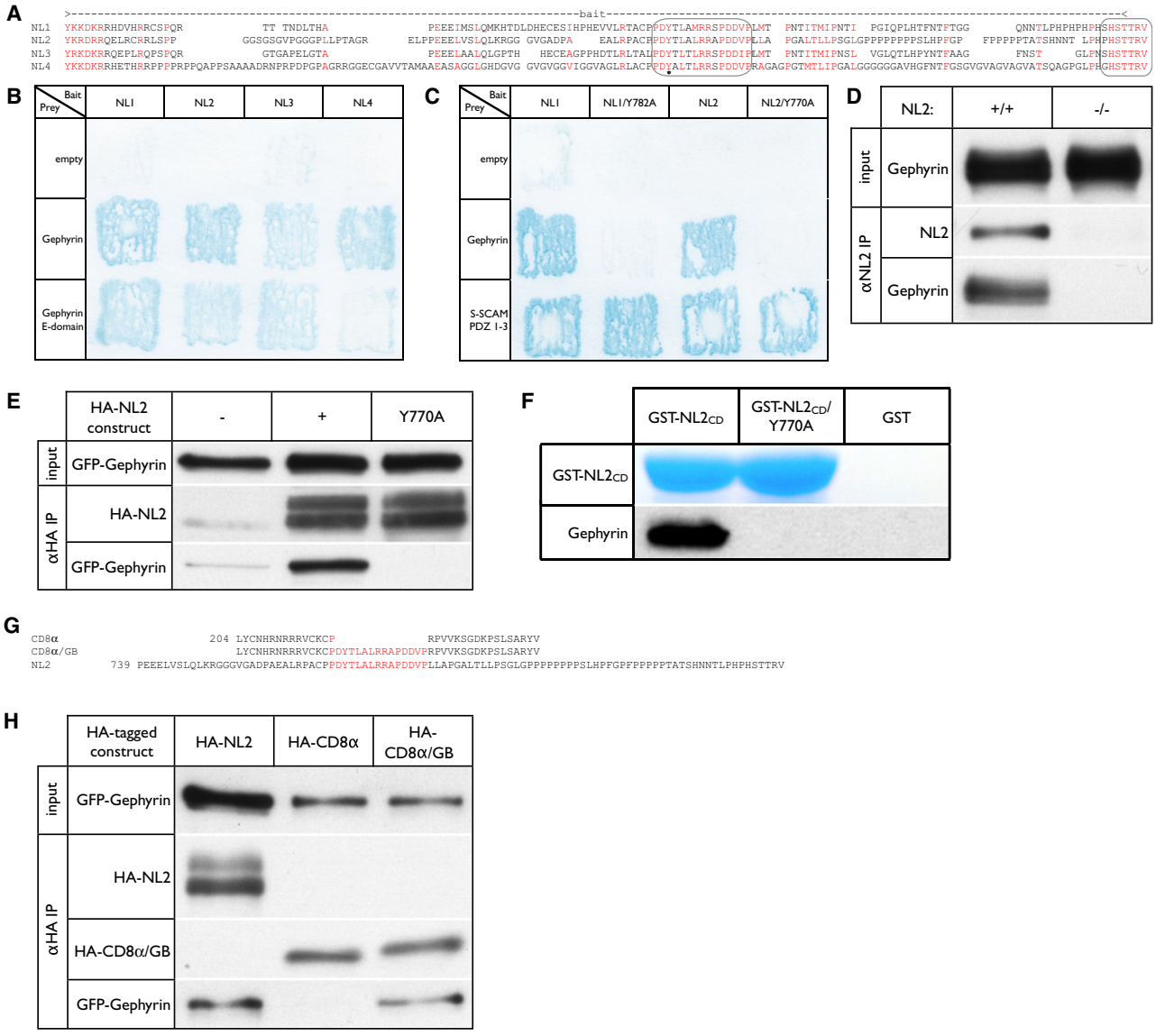

Figure 1. Neuroligins Interact with Gephyrin

(A) Alignment of the cytoplasmic domains of the four rodent NLs (NL1–3 from rat and NL4 from mouse). The segment of the NL2 sequence that was used as bait in the YTH screen is indicated above the alignment. Conserved residues are marked in red. The PDZ-binding and gephyrin-binding (GB) motifs are boxed. The conserved tyrosine targeted for mutation is designated with a dot.

(B) YTH assays with NL full cytoplasmic domain bait constructs versus gephyrin full-length and E-domain (residues 286–768) prey clones derived from the NL2 YTH screen. Gephyrin binds to all four NLs in yeast.

(C) YTH assays with NL1 and NL2 full cytoplasmic domain bait constructs and their respective NL1/Y782A and NL2/Y770A mutants versus prey constructs of full-length gephyrin and an S-SCAM fragment encompassing its three PDZ domains. Empty prey vector versus the NL bait constructs is shown in the first row as an indicator of bait autoactivity levels. The tyrosine-to-alanine substitution abolishes gephyrin binding but does not affect PDZ domain interactions.

(D) IP of endogenous NL2 from crosslinked brain samples of wild-type (+/+) or *NL2*$^{-/-}$ mice (−/−). After linker cleavage, input (0.37%) and immunoprecipitate (30%) samples were examined for endogenous gephyrin and NL2. Gephyrin is in complex with NL2 in the brain.

(E) IP of HA epitopes from crosslinked samples of COS7 cells coexpressing GFP-gephyrin along with empty vector, HA-NL2, or HA-NL2/Y770A. After linker cleavage, HA- and GFP-tagged proteins were examined in input (0.15%) and immunoprecipitate (30%) samples. GFP-gephyrin interacts with HA-NL2 but not the Y770A mutant in nonneuronal cells.

(F) Pulldown of recombinant His-gephyrin E-domain (residues 316–736) by recombinant GST-tagged NL2 cytoplasmic domain (GST-NL2$_{CD}$, left lane), GST-NL2$_{CD}$/Y770A cytoplasmic domain (center lane), or GST alone (right lane). After SDS-PAGE, GST-tagged proteins were visualized by Coomassie staining and coprecipitating His-gephyrin E-domain by immunoblotting. The NL2 cytoplasmic domain binds the gephyrin E-domain in vitro.

(G) Alignment of the cytoplasmic domain sequence of the chimera HA-CD8α/GB with the C-terminal sequences of human CD8α and rat NL2. Numbers correspond to residue positions in the full-length protein sequences. The GB motif sequence is marked in red.

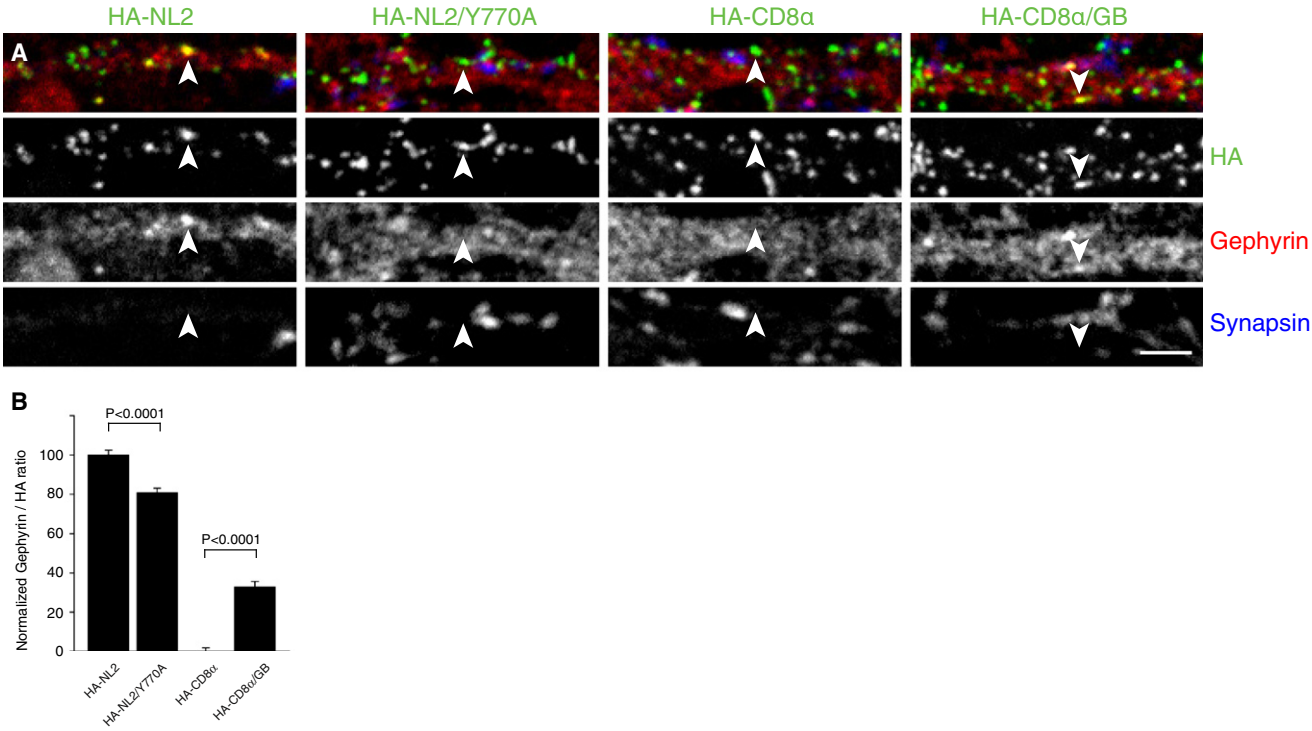

Figure 2. The Interaction of NL2 with Gephyrin Promotes Coclustering in Neurons

(A) Hippocampal neurons from *NL2*$^{-/-}$ mice were transfected at DIV7 with extracellularly HA-tagged membrane protein constructs. Acute clustering of HA (green in overlay frame) was performed at DIV8. Neurons were fixed and stained for endogenous gephyrin (red in overlay frame) and synapsin 1/2 (blue in overlay frame). The position of an extrasynaptic HA surface cluster is indicated by an arrowhead in each sample. Scale bar, 5 μm.

(B) The normalized percentage of endogenous gephyrin coclustering was measured at extrasynaptic surface clusters of HA-tagged proteins. HA-NL2: 100% ± 2.51%, 29 neurons, n = 4690 clusters; HA-NL2/Y770A: 80.8% ± 2.35%, 31 neurons, n = 5712 clusters; HA-CD8α: 0% ± 1.75%, 23 neurons, n = 4830 clusters; HA-CD8α/GB: 32.83% ± 2.8%, 12 neurons, n = 2224 clusters. HA-NL2/Y770A recruits gephyrin significantly less efficiently than HA-NL2 ($p < 0.0001$), while HA-CD8α/GB recruits gephyrin significantly more than HA-CD8α ($p < 0.0001$) in neurons.

All error bars indicate SEM.

chimera containing the NL2 GB motif recruited gephyrin significantly more than HA-CD8α, which was used to determine nonspecific association of gephyrin and HA immunoreactivities (Figure 2). These data show that the direct NL2-gephyrin interaction is involved in the mechanism that recruits gephyrin to NL2 clusters. However, quantification indicated that this interaction can only partially account for gephyrin recruitment, indicating that additional properties of NL2 may be implicated.

NL2 Is a Specific Activator of Collybistin

Collybistin has the capacity to target gephyrin to the plasma membrane. However, isoforms of collybistin detected in vivo contain an SH3 domain that renders the protein inactive in non-neuronal cells (Harvey et al., 2004; Kins et al., 2000; Papadopoulos et al., 2007). Cotransfection of a tagged variant of collybistin II containing the SH3 domain (myc-CB2$_{SH3+}$) along with GFP-gephyrin and the control transmembrane protein HA-CD8α led to the accumulation of gephyrin together with collybistin into large cytoplasmic aggregates (Figure 3A), as previously reported (Harvey et al., 2004; Kins et al., 2000). Remarkably, cotransfection of HA-NL2 dramatically affected the distribution of both gephyrin and collybistin by inducing the formation of microaggregates at the plasma membrane where all three proteins coclustered (Figure 3A and 3B). This distribution of gephyrin-collybistin complexes was indistinguishable from that observed with a tagged variant of truncated collybistin that lacks the SH3 domain (Flag-CB2$_{SH3-}$, Figure 3B, bottom row), thus rendering it constitutively active in targeting gephyrin to the plasma membrane in cell lines (Harvey et al., 2004; Kins et al., 2000). This indicates that the physiologically relevant isoforms of collybistin, i.e., those containing the SH3 domain, are activated in the presence of NL2.

In contrast to HA-NL2, the gephyrin-binding mutant HA-NL2/Y770A had only minimal capacity to induce the membrane-targeting activity of collybistin, as membrane microaggregates containing gephyrin and collybistin were rarely observed. This indicates that the interaction of NL2 with gephyrin is mechanistically coupled to the process of collybistin activation. However,

(H) IP of HA-tagged proteins from crosslinked samples of COS7 cells transfected with GFP-gephyrin along with either HA-NL2, HA-CD8α, or HA-CD8α/GB. After linker cleavage, HA- and GFP-tagged proteins were examined in input (0.37%) and immunoprecipitate (30%) samples. The GB motif promotes complex formation with GFP-gephyrin.

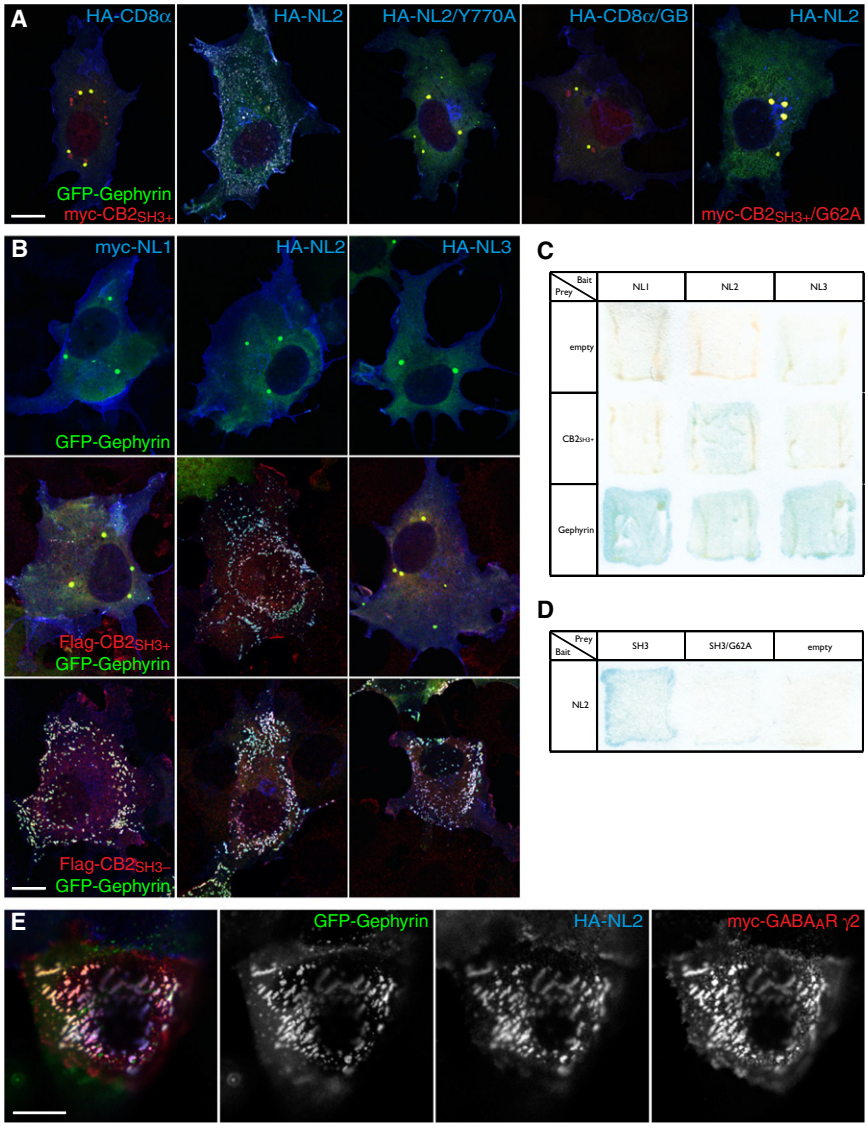

Figure 3. NL2 Specifically Activates Collybistin-Mediated Targeting of Gephyrin to the Plasma Membrane

(A) COS7 cells coexpressing GFP-gephyrin (green), myc-$CB2_{SH3+}$, or myc-$CB2_{SH3+}$/G62A (red) and either HA-CD8α, HA-NL2, HA-NL2/Y770A, or HA-CD8α/GB (blue). GFP-gephyrin and myc-$CB2_{SH3+}$ accumulate in large cytoplasmic aggregates in the absence of NL2. In the presence of HA-NL2, GFP-gephyrin and myc-$CB2_{SH3+}$ form microaggregates on the plasma membrane coclustering with HA-NL2. Mutations that disrupt the NL2-gephyrin or NL2-collybistin interactions prevent plasma membrane targeting of GFP-gephyrin and myc-$CB2_{SH3+}$. Scale bar, 20 μm.

(B) COS7 cells coexpressing myc-NL1 (left column), HA-NL2 (middle column), or HA-NL3 (blue, right column) together with GFP-gephyrin alone (green, upper row), GFP-gephyrin and Flag-$CB2_{SH3+}$ (red, middle row), or GFP-gephyrin and Flag-$CB2_{SH3-}$ (bottom row). In contrast to NL2, NL1 and NL3 do not activate collybistin. However, NLs 1–3 associate with constitutively active collybistin-gephyrin membrane microaggregates. Scale bar, 20 μm.

(C) YTH assays with $NL1\text{-}3_{CD}$ bait constructs versus empty prey vector (top row), full-length $CB2_{SH3+}$ (middle row), and gephyrin prey (bottom row). NL2, but not NL1 or NL3, interacts with collybistin.

(D) YTH assays with $NL2_{CD}$ bait construct versus the collybistin SH3 domain (SH3), SH3/G62A, and empty vector. The collybistin SH3 domain interacts with NL2. The collybistin G62A mutation hinders this interaction.

(E) HEK293 FT cells coexpressing HA-NL2, GFP-gephyrin, Flag-$CB2_{SH3+}$, $GABA_AR$ α2 subunit, $GABA_AR$ β3 subunit, and myc-$GABA_AR$ γ2 subunit were fixed and stained without permeabilizing for surface labeling of HA-NL2 (blue in overlay frame) and myc-$GABA_AR$ (red in overlay frame). Cytoplasmic GFP-gephyrin fluorescence was also detected (green in overlay frame). Clusters in which all components are enriched were observed at the plasma membrane. Scale bar, 20 μm.

the CD8α chimera containing the GB motif (HA-CD8α/GB) was not able to substitute for HA-NL2 with regard to collybistin activation (Figure 3A). Thus, interaction of gephyrin with the NL2 GB motif is necessary but not sufficient to activate collybistin. Together these data indicate that the molecular events leading to collybistin activation involve at least two distinct properties of NL2, only one of which being its binding to gephyrin.

As all NLs can bind gephyrin, we examined whether they may also have the capacity to activate collybistin. In contrast to HA-NL2, neither myc-NL1 nor HA-NL3 efficiently altered the distribution of gephyrin (Figure 3B, middle row), which remained in cytoplasmic aggregates much like in control cells lacking collybistin (Figure 3B, top row), indicating that collybistin was not activated. These data show that while all NLs bind gephyrin, NL2, but not NL1 or NL3, is a specific activator of collybistin.

We therefore examined whether NL2 may directly interact with collybistin. Indeed, in YTH assays, NL2 but not NL1 or NL3 cytoplasmic domains interacted with collybistin (Figure 3C). Importantly, the collybistin SH3 domain responsible for keeping collybistin in an inactive state was sufficient to mediate this interaction. Additionally, a G62A substitution in the SH3 domain, corresponding to a G55A substitution in the human collybistin ortholog associated with severe drug-resistant seizures and hyperekplexia (Harvey et al., 2004), disrupted NL2 binding (Figure 3D) and rendered collybistin resistant to NL2 activation in cell lines (Figure 3A). The interaction of NL2 with collybistin may thus be involved in relieving the SH3-domain-mediated inhibition of collybistin and consequently regulate membrane targeting of the gephyrin scaffold.

The collybistin variant lacking the inhibitory SH3 domain (Flag-$CB2_{SH3-}$) targets gephyrin to plasma membrane microaggregates regardless of the presence of NL2 (Harvey et al., 2004; Kins et al., 2000), indicating that it functions as a constitutively active isoform. The association of NLs with

gephyrin-collybistin membrane aggregates was examined independently from collybistin activation by employing this SH3– variant. Upon cotransfection of either myc-NL1, HA-NL2, or HA-NL3 with GFP-gephyrin and Flag-CB2$_{SH3-}$, any of the three NLs were spontaneously recruited to gephyrin-collybistin membrane microaggregates (Figure 3B, bottom row). This association relied on the interaction with gephyrin, since Y770A mutation of the NL2 GB motif disrupted specific coclustering as shown by fluorescence intensity correlation analysis between NL2 and gephyrin-collybistin complexes (Figure S2). Taken together, these data indicate that once collybistin has been activated, for instance by NL2 (or in the absence of the SH3 domain), all NLs have the ability to associate with membrane accumulations of gephyrin through the GB motif. However, only NL2 can bind to and activate the physiologically relevant SH3+ collybistin isoforms and induce the translocation of gephyrin-collybistin complexes to the plasma membrane.

Reconstitution of Self-Organizing GABAergic "Postsynaptic" Elements

Aggregated gephyrin is sufficient to recruit glycine receptors but not GABA$_A$ receptors in nonneuronal cells (Meyer et al., 1995). We examined whether the NL2-gephyrin-collybistin membrane complex may be sufficient to recruit GABA$_A$ receptors.

The GABA$_A$ receptor subunits α2, β3, and myc-tagged γ2 were cotransfected with GFP-gephyrin, Flag-CB2$_{SH3+}$, and HA-NL2 in nonneuronal cells (Figure 3E). Postfixation surface immunostaining for the myc epitope was employed to label fully assembled GABA$_A$ receptors since the γ2 subunit has been shown to traffic to the surface only upon coassembly with α and β GABA$_A$ receptor subunits (Connolly et al., 1996). Postfixation HA surface immunostaining was used to label NL2 on the plasma membrane, while gephyrin was visualized through GFP fluorescence. Coexpression of collybistin can be inferred by the presence of GFP-gephyrin membrane microaggregates characteristic of gephyrin-collybistin complexes.

In cotransfected cells, we observed GABA$_A$ receptors to be spontaneously coclustered with membrane microaggregates (Figure 3E), reflecting the formation of discrete plasma membrane specializations containing receptor, scaffolding, and adhesion proteins, as such resembling basic GABAergic postsynaptic elements. It remains unclear whether GABA$_A$ receptors are recruited through interactions with gephyrin (Tretter et al., 2008) or through association with NL2 (Dong et al., 2007). Nevertheless, omission of either NL2, gephyrin, or collybistin from the heterologous system resulted in the collapse of the coclustered structure; cytoplasmic protein constituents segregated into large aggregates, while membrane protein constituents diffusely distributed throughout the plasma membrane. Together, these data indicate that gephyrin-collybistin complexes activated by, and coclustered with, NL2 are sufficient for the recruitment of GABA$_A$ receptors at plasma membrane clusters.

NL2 Is Essential for Both GABAergic and Glycinergic Transmission In Vivo

The integrity of the gephyrin scaffold is important for both glycinergic (Feng et al., 1998) and GABAergic transmission (Kneussel et al., 1999). To examine the role of NL2 in synaptic inhibition, we studied the effect of NL2 deletion on synaptic transmission in mice. *NL2*$^{-/-}$ mice have the same life span and survival rates as wild-type littermates, and levels of key synaptic proteins are unchanged (Figure S3). Newborn *NL2*$^{-/-}$ mice, however, exhibit irregular breathing patterns (Figure S4A–S4C). This prompted us to examine synaptic transmission in the neuronal network generating the respiratory rhythm in the ventrolateral medulla (RVLM; Richter and Spyer, 2001), where both GABAergic and glycinergic components of synaptic inhibition are prevalent and which we had previously analyzed in NL1/2/3 triple-mutant mice (Varoqueaux et al., 2006).

Whole-cell patch-clamp recordings in acute brainstem slices containing the RVLM revealed that absence of NL2 causes a severe depression in both the frequency and amplitude of spontaneous and evoked network activity (Figures S4D–S4I). In order to identify the synaptic basis of this phenotype, excitatory (EPSC) and inhibitory (IPSC) postsynaptic currents were dissected pharmacologically. Silencing of glutamatergic transmission revealed strong deficits in synaptic inhibition in the *NL2*$^{-/-}$ brainstem, with a 3-fold reduction in the frequency of spontaneous inhibitory events (Figure S5) and a reduction in the amplitude and an increase in the failure rate of inhibitory responses to evoked stimulation (Figures 4A–4C, 4F, and 4G). Glutamatergic transmission, instead, remained unaffected in the absence of NL2 (Figures 4J–4L), highlighting the specificity of NL2 function in synaptic inhibition in vivo. As both excitatory and inhibitory total synapse numbers in the RVLM were unaltered in mutant animals (Figure S6), reduced inhibitory transmission in the *NL2*$^{-/-}$ brainstem cannot be attributed to a loss of synapses per se, but rather to defects of the synaptic apparatus in a population of inhibitory synapses.

Pharmacological segregation of inhibitory transmission into GABAergic and glycinergic components showed that deletion of NL2 was detrimental to both. Pharmacologically isolated GABAergic spontaneous IPSCs exhibited a 6-fold reduction in frequency and a 28% reduction in amplitude in *NL2*$^{-/-}$ animals as compared to wild-type littermates (Figure 4B). These deficits were essentially mirrored in glycinergic currents (Figure 4F). To examine this effect further, miniature currents (mIPSCs) were recorded after blocking action potential-mediated network activity with TTX. Both GABAergic and glycinergic mIPSCs were perturbed in frequency and amplitude (Figures 4C and 4G). Interestingly, analysis of mIPSC kinetics revealed a shift toward slower-peaking events in *NL2*$^{-/-}$ mutants (Figures 4D and 4H), while excitatory event kinetics remained unaltered (Figure 4M). In conjunction with the reduction in mIPSC frequency, this indicates a specific loss of rapid-onset inhibitory events in *NL2*$^{-/-}$ animals.

In order to directly assess deficits in the postsynaptic cell independently from the presynaptic component, receptor agonists were locally applied via extracellular pressure ejection onto the recorded neurons. Postsynaptic currents recorded during local application of GABA$_A$ receptor agonist showed a 3-fold reduction in response amplitude in *NL2*$^{-/-}$ neurons compared to wild-type controls (Figure 4E). Application of glycine revealed a 2-fold reduction in glycine receptor responses in mutant neurons (Figure 4I), while glutamate application induced similar responses in either genotype (Figure 4N). These results point to a specific deficit in

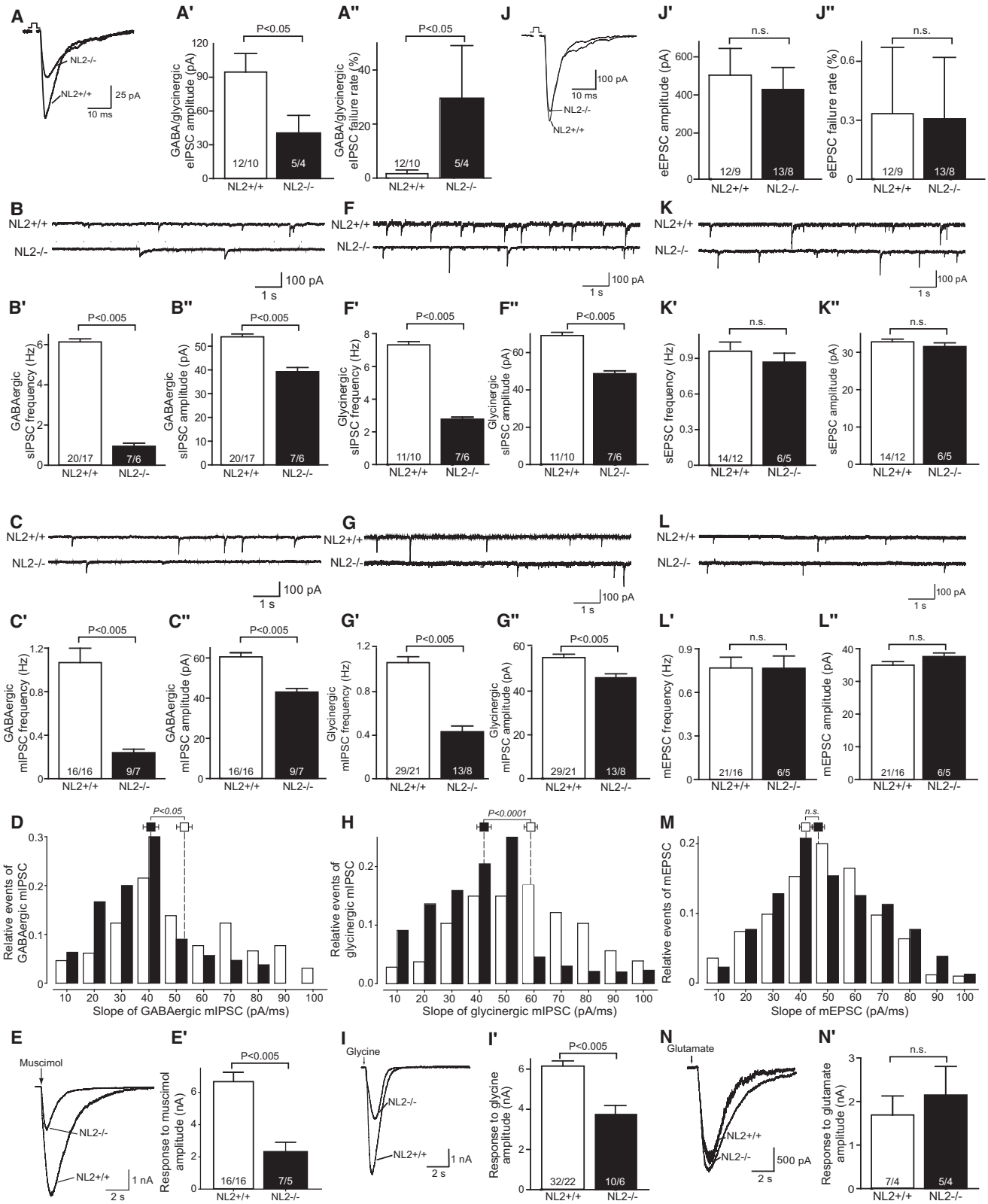
A
NL2-/-
NL2+/+
25 pA
10 ms
A'
P<0.05
GABA/glycinergic eIPSC amplitude (pA)
12/10
5/4
NL2+/+
NL2-/-
A''
P<0.05
GABA/glycinergic eIPSC failure rate (%)
12/10
5/4
J
100 pA
10 ms
NL2-/-
NL2+/+
J'
n.s.
eEPSC amplitude (pA)
12/9
13/8
J''
n.s.
eEPSC failure rate (%)
12/9
13/8
B
NL2+/+
NL2-/-
100 pA
1 s
F
K
B'
P<0.005
GABAergic sIPSC frequency (Hz)
20/17
7/6
B''
P<0.005
GABAergic sIPSC amplitude (pA)
20/17
7/6
F'
P<0.005
Glycinergic sIPSC frequency (Hz)
11/10
7/6
F''
P<0.005
Glycinergic sIPSC amplitude (pA)
11/10
7/6
K'
n.s.
sEPSC frequency (Hz)
14/12
6/5
K''
n.s.
sEPSC amplitude (pA)
14/12
6/5
C
G
L
C'
P<0.005
GABAergic mIPSC frequency (Hz)
16/16
9/7
C''
P<0.005
GABAergic mIPSC amplitude (pA)
16/16
9/7
G'
P<0.005
Glycinergic mIPSC frequency (Hz)
29/21
13/8
G''
P<0.005
Glycinergic mIPSC amplitude (pA)
29/21
13/8
L'
n.s.
mEPSC frequency (Hz)
21/16
6/5
L''
n.s.
mEPSC amplitude (pA)
21/16
6/5
D
P<0.05
Relative events of GABAergic mIPSC
Slope of GABAergic mIPSC (pA/ms)
H
P<0.0001
Relative events of glycinergic mIPSC
Slope of glycinergic mIPSC (pA/ms)
M
n.s.
Relative events of mEPSC
Slope of mEPSC (pA/ms)
E
Muscimol
NL2-/-
NL2+/+
1 nA
2 s
E'
P<0.005
Response to muscimol amplitude (nA)
16/16
7/5
I
Glycine
NL2-/-
NL2+/+
1 nA
2 s
I'
P<0.005
Response to glycine amplitude (nA)
32/22
10/6
N
Glutamate
NL2+/+
NL2-/-
500 pA
2 s
N'
n.s.
Response to glutamate amplitude (nA)
7/4
5/4

functional $GABA_A$ and glycine receptors in $NL2^{-/-}$ neurons. Taken together, they indicate that NL2 is essential for the function of the postsynaptic receptor apparatus of inhibitory but not excitatory synapses in the brain, while the phenotype of $NL2^{-/-}$ mice with regard to synaptic inhibition is pleiotropic in terms of its effect on both GABAergic and glycinergic transmission.

NL2 Is Necessary for the Postsynaptic Recruitment of Gephyrin at Perisomatic but Not Dendritic Sites

Our cell-line data indicate that NL2 can function together with collybistin to recruit gephyrin to the plasma membrane, while electrophysiological recordings show that NL2 is necessary for the proper function of both gephyrin-dependent receptor systems, $GABA_A$ and glycine. We thus examined the role of NL2 in the postsynaptic clustering of gephyrin during synaptogenesis and in the adult brain. Dissociated hippocampal neurons in culture from $NL2^{-/-}$ or wild-type littermate mice were immunolabeled for endogenous gephyrin and synapsin, a marker of presynaptic innervation (Figure 5A). In immature wild-type neurons (day in vitro [DIV] 4), gephyrin accumulated at postsynaptic sites infrequently, while it was prominently detected in cytoplasmic aggregates in the soma. Upon development of the culture (DIV16), gephyrin localized predominantly postsynaptically while cytoplasmic aggregates were absent.

Strikingly, in neurons lacking NL2, gephyrin cytoplasmic aggregates often persisted until the late stages of the culture, while postsynaptic gephyrin clustering at perisomatic synapses was severely impaired, despite neurons being properly innervated (Figure 5). Interestingly, and in contrast to our observations at neuronal somata, dendritic postsynaptic gephyrin clusters remained unaffected in $NL2^{-/-}$ neurons (Figure 5D), indicating a difference in the gephyrin recruitment mechanisms at the somatic versus dendritic compartment.

In the CA1 region of the adult hippocampus, deletion of NL2 led to a phenotype that correlates with the observations in dissociated neurons. The number of gephyrin puncta were specifically reduced in the *stratum* (*str.*) *pyramidale*, which contains pyramidal cell somata, despite unaltered inhibitory innervation as assessed by vesicular inhibitory amino acid transporter (VIAAT) immunolabeling. Conversely, gephyrin puncta remained unaffected in the *str. radiatum* where synapses form onto pyramidal cell dendrites (Figures 6A–6C). These effects of NL2 deletion on gephyrin were mirrored in $GABA_A$ receptors, as the number of $\gamma 2$ subunit puncta was reduced following a similar layer-specific pattern (Figure S7). Concomitant to the reduction of gephyrin puncta, large cytoplasmic aggregates of gephyrin were observed at the apical pole of $NL2^{-/-}$ pyramidal cell somata close to the interface with the *str. oriens* (Figures 6D–6E), further corroborating our findings in culture.

To assess the effects of the selective disruption observed at perisomatic GABAergic synapses in the hippocampus of $NL2^{-/-}$ mice, electrophysiological recordings were performed on acute hippocampal slices from adult animals. In the absence of NL2, 2-fold reductions in GABAergic sIPSC and mIPSC frequency were observed together with marginal reductions in peak amplitudes (Figures 6F–6K). To examine whether these reductions in frequency could represent the specific loss of perisomatic events, we analyzed mIPSC kinetics, since perisomatic events display faster onset as compared to dendritic events (Miles et al., 1996). In the hippocampus, as in the brainstem, mIPSP kinetics exhibited a shift toward events with slower onset in $NL2^{-/-}$ mice. The mean slope of event onset was reduced 2-fold in mutant animals (Figure 6K), supporting the notion of a selective loss of fast-onset perisomatic events. Thus morphological and electrophysiological data collectively document the mistargeting of somatic gephyrin and the concomitant perturbation of perisomatic inhibition in the NL2-deficient hippocampus.

Disruption of postsynaptic gephyrin clusters in hippocampal neurons is also a feature of the collybistin knockout mouse (Papadopoulos et al., 2007). This similarity of phenotypes between NL2 and collybistin mutant mice supports a general functional relationship of the two proteins. In collybistin mutant mice, however, perturbation of postsynaptic gephyrin was not limited to perisomatic clusters, while postsynaptic targeting of NL2 was unaltered (Figure S8). These data indicate that NL2 functions upstream of collybistin in the pathway leading to postsynaptic gephyrin clustering at perisomatic synapses.

DISCUSSION

In this study, we examined the function of NL2 at the inhibitory postsynapse and its role in synaptic transmission. We show

Figure 4. NL2 Is Required for Proper GABAergic and Glycinergic but Not Glutamatergic Transmission in the Brainstem

Representative recordings of (A) evoked inhibitory postsynaptic currents (eIPSC) and (J) evoked excitatory postsynaptic currents (eEPSC) from neurons in the hypoglossus nucleus at postnatal day (P) 2–4. Quantification of the average amplitudes (') and failure rates ('') of evoked events in wild-type ($NL2^{+/+}$, empty bars) and $NL2^{-/-}$ (filled-in bars) neurons.

Representative recordings of (B) spontaneous GABAergic inhibitory postsynaptic currents (sIPSC), (F) glycinergic sIPSCs, and (K) glutamatergic spontaneous excitatory postsynaptic currents (sEPSCs) from neurons in the ventrolateral medulla at P2–P4. Quantification of the average frequencies (') and amplitudes ('') of spontaneous events in $NL2^{+/+}$ and $NL2^{-/-}$ neurons.

Representative recordings of (C) GABAergic miniature inhibitory postsynaptic currents (mIPSC), (G) glycinergic mIPSCs, and (L) glutamatergic excitatory postsynaptic currents (mEPSC) from neurons in the ventrolateral medulla at P2–P4. Average frequencies (') and amplitudes ('') of miniature events in $NL2^{+/+}$ and $NL2^{-/-}$ neurons. Onset kinetics expressed as normalized histograms of rise slopes (peak amplitude in pA over time to onset in ms) of (D) GABAergic mIPSCs, (H) glycinergic mIPSCs, and (M) glutamatergic mEPSCs in $NL2^{+/+}$ and $NL2^{-/-}$ neurons. Mean values and the significance of their difference are indicated by squares positioned relative to the x axis of the histogram.

Sample traces and average amplitudes (') of postsynaptic responses to local extracellular application of (E) the $GABA_A$ agonist muscimol (5 mM), (I) glycine (5 mM), and (N) glutamate (5 mM) in $NL2^{+/+}$ and $NL2^{-/-}$ neurons in the ventrolateral medulla at P2–P4.

Deletion of NL2 causes deficits in both GABAergic and glycinergic transmission (left and center columns) with a loss of receptors on the postsynaptic cell. Glutamatergic transmission (right column) remained unhindered. Numbers within the bar graphs indicate the number of neurons/mice tested for each genotype.

All error bars indicate SEM.

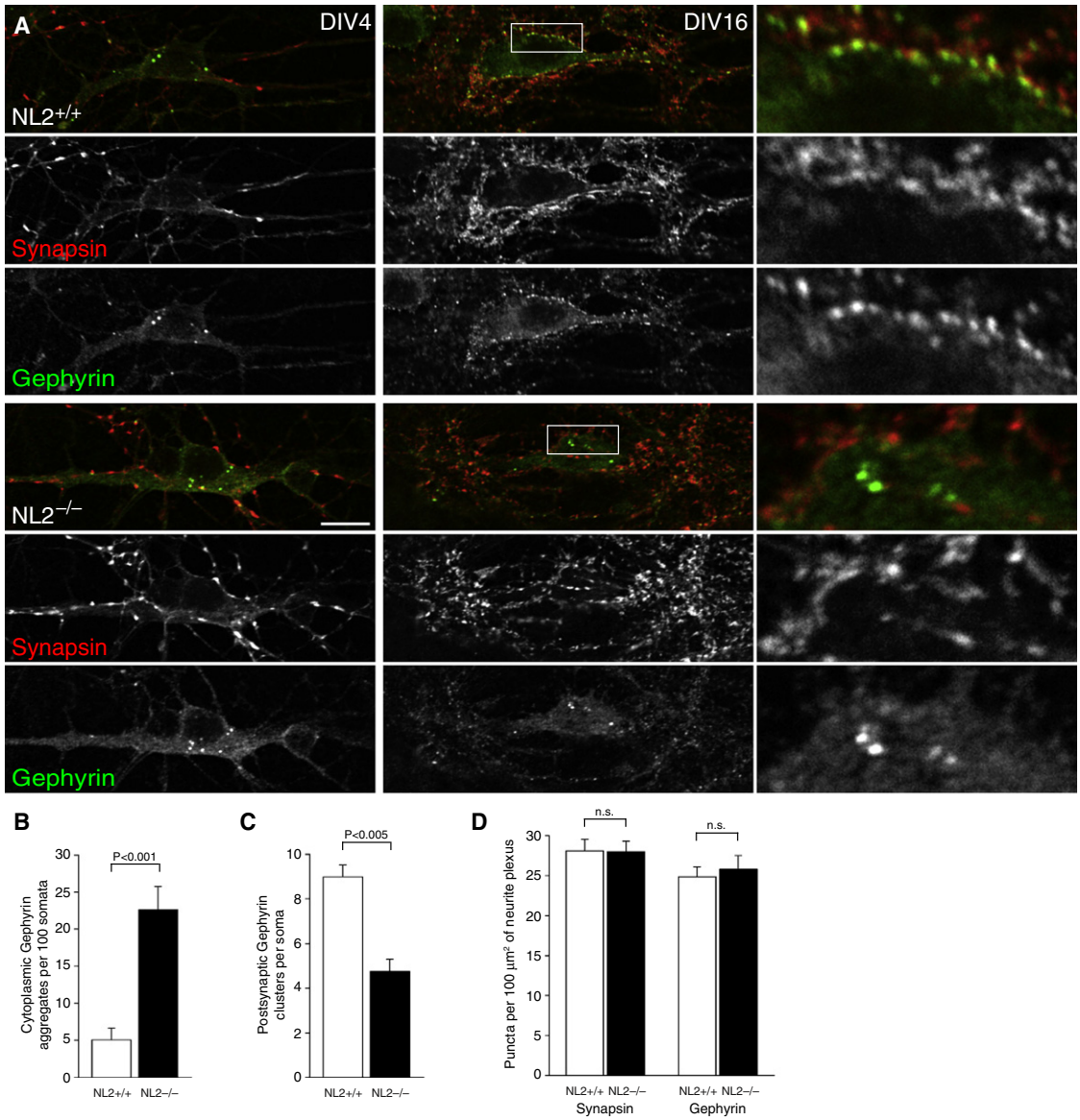

Figure 5. *NL2*$^{-/-}$ Neurons in Culture Display Deficits in Postsynaptic Targeting of Gephyrin at Perisomatic Synapses

(A) Hippocampal neurons from wild-type (*NL2*$^{+/+}$) or *NL2*$^{-/-}$ mice at DIV4 and DIV16 were immunolabeled for endogenous synapsin 1/2 (red in overlay frame) and gephyrin (green in overlay frame). Scale bar: 10 μm, main panels; 2.2 μm, insets.

(B) Quantification of the occurrence of cytoplasmic aggregates of gephyrin per 100 somata at DIV16. *NL2*$^{+/+}$: 5.03 ± 1.6, n = 9 mice, 412 neurons; *NL2*$^{-/-}$: 22.6 ± 3.2, n = 7 mice, 307 neurons. Cytoplasmic gephyrin aggregates appeared significantly more often in neurons from mice lacking NL2 ($p < 0.001$).

(C) Quantification of the number of postsynaptic gephyrin clusters on the somatic region per neuron at DIV16. *NL2*$^{+/+}$: 8.98 ± 0.95, n = 9 mice, 370 neurons; *NL2*$^{-/-}$: 4.75 ± 0.54, n = 7 mice, 267 neurons. Neurons lacking NL2 had significantly less clusters of postsynaptic gephyrin in the somatic region ($p < 0.005$).

(D) Quantification of the density of synapsin and gephyrin puncta on neurites (puncta per 100 μm^2 of neuritic plexus) at DIV16. *NL2*$^{+/+}$: synapsin 28.09 ± 1.46, gephyrin 24.84 ± 1.27, n = 9 mice, 2953 μm^2 of neurite plexus measured. *NL2*$^{-/-}$: synapsin 27.98 ± 1.32, gephyrin 25.8 ± 1.72, n = 7 mice, 1945 μm^2 of neurite plexus measured. No differences in the density of synapsin or gephyrin puncta were observed in the neurites of *NL2*$^{+/+}$ and *NL2*$^{-/-}$ neurons.

All error bars indicate SEM.

that NL2 interacts with two major proteins known to be required for the differentiation of inhibitory postsynapses: gephyrin and collybistin. We unraveled a molecular chain of events where NL2 functions as a postsynaptic organizer at contact sites of inhibitory terminals. Our findings also establish an unexpected specificity of NL2 function at perisomatic synapses.

Specificities of NL Postsynaptic Interactions

Inhibitory synapses have a distinct scaffolding system dominated by the protein gephyrin, which is crucial for postsynaptic clustering of both $GABA_A$ and glycine receptors (Essrich et al., 1998; Feng et al., 1998; Kirsch et al., 1993; Kneussel et al., 1999). Despite its inhibitory synapse-specific localization and

multiple interactions with synaptic and cytoskeleton-associated proteins (reviewed in Fritschy et al., 2008), gephyrin has, until now, not been shown to bind transsynaptic complexes. We have now identified NL2 as the synaptic adhesion protein interaction partner of gephyrin, documenting the interaction in vitro, in yeast, nonneuronal cell lines, and the brain.

NL2 interacts with the E domain of gephyrin. This domain is crucial for homodimerization (Sola et al., 2004) and for interactions with several proteins, including the glycine receptor β subunit (Meyer et al., 1995) and collybistin (Harvey et al., 2004). On the NL2 side, a small cytoplasmic motif was found to be necessary and sufficient for interaction with gephyrin. Surprisingly, this novel GB motif is conserved in all NLs and can thus not account for the differential synaptic specificities of NLs.

NL2 is found exclusively and consistently at inhibitory synapses (Varoqueaux et al., 2004). Conversely, NL1 is primarily localized at excitatory synapses (Song et al., 1999), while NL3 appears to localize to a subset of both excitatory and inhibitory synapses (Budreck and Scheiffele, 2007). The localization of NL4 has yet to be examined. This selective localization of NL paralogs at distinct synapses appears to be mediated by transsynaptic interactions with diverse NX isoforms on presynaptic terminals (Chih et al., 2006; Kang et al., 2008). Given that PDZ- and gephyrin-binding domains that accommodate both excitatory and inhibitory scaffolds are ubiquitous to all NLs, a molecular mechanism conveying this specificity to the postsynaptic scaffold and receptors had remained elusive. We observed that NL2, but not NL1 or NL3, has the capacity to interact with and activate collybistin, inducing the targeting of gephyrin-collybistin to the plasma membrane (Figure 3). These data provide evidence for a functional specificity of NL2 at the inhibitory postsynapse, not shared by NL1 or NL3.

Collybistin is found in complex with gephyrin, can translocate it to the plasma membrane (Kins et al., 2000), and is required for synaptic targeting of gephyrin in vivo (Papadopoulos et al., 2007). The mechanism through which collybistin functions is thought to involve binding to membrane lipids through its Pleckstrin homology domain (Harvey et al., 2004; Kalscheuer et al., 2009). However, endogenous collybistin variants contain a regulatory SH3 domain that inhibits their membrane-targeting function in nonneuronal cells (Harvey et al., 2004; Kins et al., 2000), implying that a neuron-specific factor must activate collybistin by relieving SH3-mediated inhibition. We find that NL2 has the capacity to function as such.

A plausible mechanism of collybistin activation entails the interaction of NL2 with the collybistin SH3 domain (Figure 3D). A G55A substitution in human collybistin is associated with clinical manifestations (epilepsy and hyperekplexia) that point to deficits in both GABAergic and glycinergic transmission (Harvey et al., 2004). The homologous rodent collybistin mutation G62A disrupted interaction with NL2 in yeast (Figure 3D), rendered collybistin irresponsive to NL2 activation in nonneuronal cells (Figure 3A), and obstructed postsynaptic targeting of $GABA_A$ receptors and gephyrin in cultured neurons (Harvey et al., 2004). Further investigation could clarify whether the observed perturbation of the NL2-collybistin interaction results in faulty postsynaptic differentiation as a contributing factor in the manifestations of epilepsy and hyperekplexia associated with the human mutation.

Based on these observations, we propose that the capacity of NL2 to function as a collybistin activator is a key determinant of its specificity for inhibitory synapses. The finding that all NLs can bind both excitatory and inhibitory scaffolds and can associate with preformed gephyrin-collybistin microaggregates (Figure 3B, bottom row) may explain previous reports of deviations from the proposed specificity, including instances where NL3 or minor NL1 splice variants associate with inhibitory synapses (Budreck and Scheiffele, 2007; Chih et al., 2006), or the promiscuous effects on both excitatory and inhibitory synapses in cases of overexpression or knock-down of different NLs in hippocampal cultures (Chih et al., 2005; Levinson et al., 2005). The present data thus reconcile the rather nonspecific effects of NLs in vitro and the striking specificity they exhibit in vivo. Additionally, they accommodate for the potential function of diverse NLs at subsets of inhibitory synapses.

Assembly of the Inhibitory Postsynaptic Apparatus

The transsynaptic adhesion complex formed by NLs and NXs is sufficient to induce synaptic differentiation (Dean et al., 2003; Graf et al., 2004; Scheiffele et al., 2000). At the inhibitory postsynapse, it is well established that clustering of gephyrin is sufficient to recruit glycine receptors (Fritschy et al., 2008). We demonstrate here that the spontaneous assembly of NL2-gephyrin-collybistin complexes at plasma membrane sites of nonneuronal cells is sufficient to cluster $GABA_A$ receptors as well (Figure 3E). This cell-autonomous reconstitution of inhibitory "postsynaptic" elements in a heterologous system serves to exemplify that these proteins are sufficient for basic postsynaptic organization.

Gene-deletion experiments provide insights into the sequence by which these key proteins operate in the postsynaptic differentiation pathway. Deletion of either NL2 (Figures 5, 6, and S7) or collybistin (Papadopoulos et al., 2007) perturbs the postsynaptic recruitment of gephyrin and $GABA_A$ receptors. However, the postsynaptic localization of NL2 is not affected by collybistin deletion or by the subsequent loss of postsynaptic gephyrin and receptors (Figure S8). Thus, genetic evidence indicates that NL2 acts upstream of scaffold deployment in the pathway leading to postsynaptic differentiation at inhibitory synapses.

Based on these data, we propose a model of inhibitory postsynaptic differentiation according to which NL2 accumulates across GABAergic or glycinergic presynaptic terminals to form nucleation sites that spatially demarcate the deployment of the gephyrin scaffold at the plasma membrane (Figure 7). At these sites, NL2 specifically activates collybistin through a mechanism involving NL2-gephyrin and NL2-collybistin interactions. This putative tripartite complex induces the local activation of collybistin and consequent tethering of the scaffolding complex to the plasma membrane, in effect nucleating gephyrin recruitment at the postsynaptic membrane of nascent inhibitory synapses. According to this model, the collybistin SH3 domain would prevent gephyrin-collybistin translocation at extrasynaptic or excitatory synaptic sites that lack NL2, implicating this domain in conferring the inhibitory synapse-specific localization of the gephyrin scaffold. The deployment of the gephyrin-collybistin complex at sites of NL2 clusters would form a core postsynaptic scaffold that accommodates inhibitory receptors, ultimately

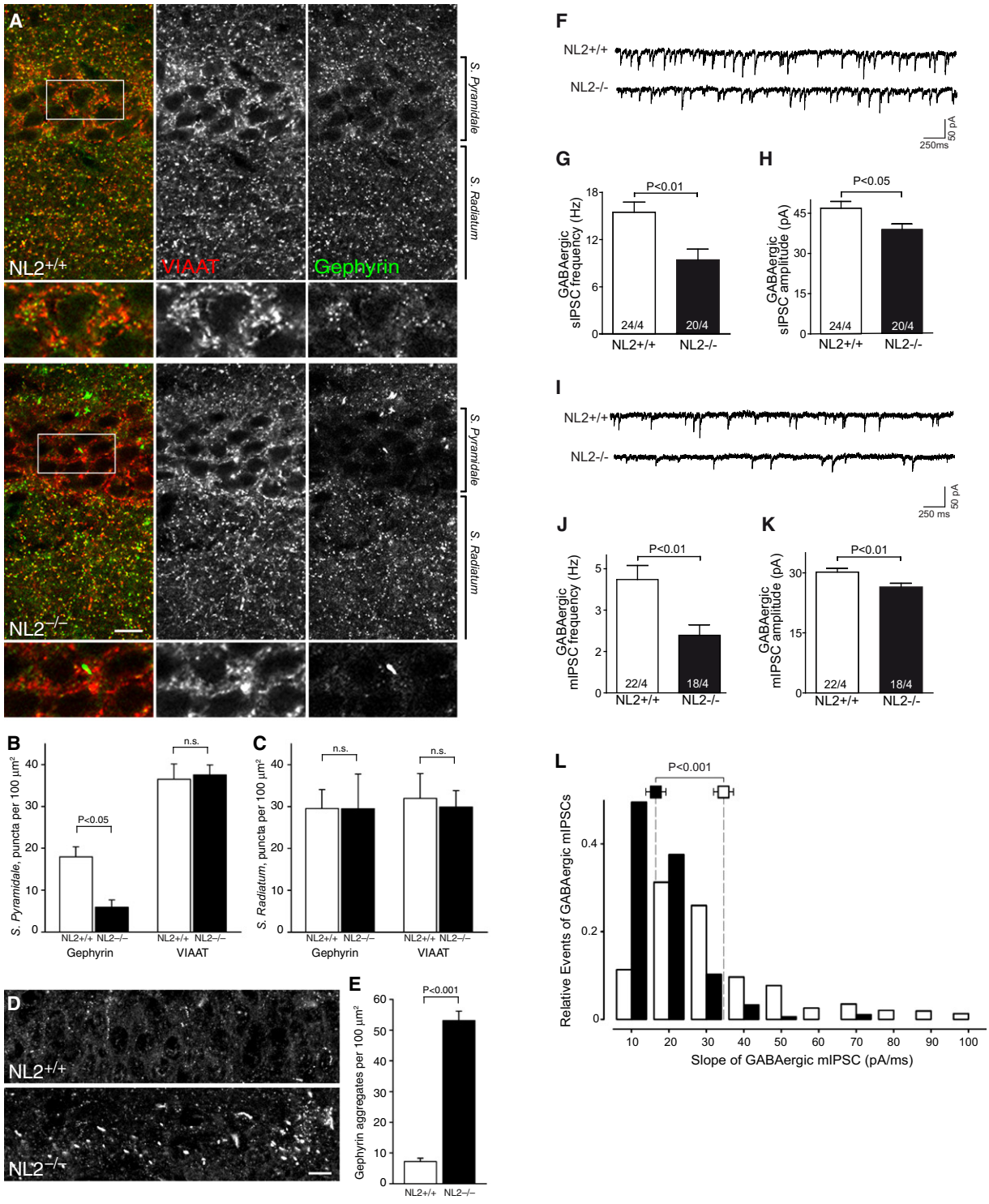

Figure 6. GABAergic Transmission and Postsynaptic Differentiation Are Perturbed at Perisomatic Synapses in the Hippocampus of *NL2*$^{-/-}$ Mice

(A) Single-plane confocal micrographs of frontal brain sections showing segments of the *str. pyramidale* and *str. radiatum* of the CA1 region of the hippocampus from adult wild-type (*NL2*$^{+/+}$) and *NL2*$^{-/-}$ mice immunolabeled for endogenous VIAAT (red in overlay frame) and gephyrin (green in overlay frame). Scale bar, 10 µm. Quantification of gephyrin and VIAAT punctum density in the *str. pyramidale* (B) and *str. radiatum* (C) (puncta per 100 µm^2). gephyrin: *str. pyramidale NL2*$^{+/+}$ 18 ± 2.4, *NL2*$^{-/-}$ 5.9 ± 1.7 ($p < 0.05$); *str. radiatum NL2*$^{+/+}$ 30 ± 4.5, *NL2*$^{-/-}$ 29.5 ± 8.3. *NL2*$^{+/+}$ n = 3 mice; *NL2*$^{-/-}$ n = 3 mice. VIAAT: *str. pyramidale NL2*$^{+/+}$ 36.5 ± 3.6, *NL2*$^{-/-}$ 37.6 ± 2.4; *str. radiatum NL2*$^{+/+}$ 32 ± 5.9, *NL2*$^{-/-}$ 29.9 ± 3.9. *NL2*$^{+/+}$ n = 3 mice; *NL2*$^{-/-}$ n = 5 mice.

recruiting them in apposition to inhibitory presynaptic terminals (Figure 7).

Levels of Synaptic Specificity

NLs exhibit transmitter-specific functions. Single deletion of NL1 was shown to affect glutamatergic transmission in the hippocampus, while NL2 deletion affected inhibitory transmission in the cortex (Chubykin et al., 2007) and retina (Hoon et al., 2009). In the present study, we examined the hippocampus and brainstem and found that deletion of NL2 specifically perturbs synaptic inhibition, affecting both GABAergic and glycinergic transmission in the respiratory brainstem and causing irregular breathing patterns in young *NL2*$^{-/-}$ mice.

To interpret the pleiotropy of the phenotype, which concerns both inhibitory transmitter systems, one may postulate that NL2 equips the postsynaptic membrane with $GABA_A$ and glycine receptors through independent mechanisms. A more straightforward interpretation is to consider NL2 a component of a recruitment pathway common to both receptor types. As gephyrin represents a common node in both $GABA_A$ and glycine receptor recruitment, we propose that deletion of NL2 leads to deficits in both GABAergic and glycinergic transmission through the disruption of the postsynaptic targeting of the gephyrin scaffold.

Observation of endogenous gephyrin in *NL2*$^{-/-}$ neurons confirmed that gephyrin requires NL2 for proper postsynaptic targeting and additionally uncovered a previously unanticipated specificity. In the absence of NL2, pyramidal neurons exhibit ectopic gephyrin in cytoplasmic aggregates and lose postsynaptic gephyrin specifically at perisomatic but not at dendritic synapses, as seen in dissociated neurons (Figure 5) and brain sections (Figure 6). Perisomatic but not dendritic $GABA_A$ receptor clusters were also selectively affected (Figure S8). Electrophysiological recordings confirmed the loss of a subset of inhibitory events in the absence of NL2 (Figures 4 and 6) and revealed that this loss primarily concerns rapid-onset events (Figures 4D, 4H, and 6L). Since somatic events have steeper rise kinetics (Miles et al., 1996) as a result of their proximity to the recording electrode, both electrophysiological and morphological evidence points to a specific loss of events that mediate perisomatic inhibition.

NL2$^{-/-}$ mice may thus serve as a tool to examine the role of perisomatic inhibition in brain function and behavior. A recent study reported that *NL2*$^{-/-}$ mice exhibit anxiety-like behavior (Blundell et al., 2009). Together with our findings, these data indicate that anxiety may result from the perturbation of perisomatic inhibition. This interpretation correlates with the finding that the anxiolytic effects of benzodiazepines are mediated through augmentation of $GABA_A$ α2 subunit-containing receptors (Löw et al., 2000), which are specifically enriched in a subclass of perisomatic synapses (Nusser et al., 1996). Together, these findings strongly implicate perisomatic inhibition in anxiety disorders.

Deletion of collybistin also results in the loss of the inhibitory postsynaptic apparatus in pyramidal cell somata. This indicates that NL2 and collybistin are both necessary constituents of inhibitory postsynapse assembly at perisomatic synapses of the hippocampus. However, unlike *NL2*$^{-/-}$ animals, collybistin knockout mice show indiscriminate loss of postsynaptic gephyrin clustering throughout the CA1 region of the hippocampus, displaying no subcellular specificity (Figure S8). Nonetheless, collybistin deletion displays a different kind of specificity, as it affects postsynaptic gephyrin in a region-specific manner; deficits seen in regions like the hippocampus or cortex are not apparent in regions like the spinal cord or brainstem (Papadopoulos et al., 2007).

Mouse genetic evidence argues in favor of selectivity in the function of both NL2 and collybistin. However, expression patterns of the proteins are not the mediators of this selectivity as both are broadly distributed in the CNS. Indeed, apart from the fact that NL2 is present at both perisomatic and dendritic synapses (Varoqueaux et al., 2004) and that collybistin is expressed throughout the brain (Kneussel et al., 2001), there is additional indirect evidence for a widespread function of these proteins. Exogenous clustering of NL2 results in the recruitment of gephyrin at both somatic and dendritic sites (Figure S1). On the collybistin side, the human G55A mutation is associated with symptoms of epilepsy and hyperekplexia pointing to dysfunctions in inhibition in the brain as well as the spinal cord. It is thus likely that both proteins function in a wide range of inhibitory synapses. However, the corresponding knockout phenotypes clearly show that other proteins can compensate the loss of NL2 or collybistin in subsets of inhibitory synapses and point to differential redundancy as being a component of synapse specificity.

At excitatory synapses, the recent finding that members of the LRRTM family of adhesion proteins have layer-specific distributions (Linhoff et al., 2009) sets a precedent for differential redundancy of factors that drive postsynaptic differentiation (Brose, 2009). In view of the present findings, the notion of differential redundancy seems to also be relevant for inhibitory synapses, raising the possibility of additional yet unidentified factors with distinct specificities being implicated. The diversity of synaptic inhibition may thus be established by the interplay of several

(D) Epifluorescence micrographs showing the *str. pyramidale* of the CA1 region of the hippocampus from adult *NL2*$^{+/+}$ and *NL2*$^{-/-}$ mice immunolabeled for endogenous gephyrin.

(E) Quantification of large gephyrin aggregates in the *str. pyramidale* (aggregates per 100 μm^2): *NL2*$^{+/+}$ 7.2 ± 1.1, n = 5 mice; *NL2*$^{-/-}$ 53.1 ± 3.1, n = 5 mice; ($p < 0.001$).

(F) Representative recordings of spontaneous GABAergic inhibitory postsynaptic currents (sIPSC) from CA1 pyramidal neurons in acute hippocampal slices from adult *NL2*$^{+/+}$ (empty bars) and *NL2*$^{-/-}$ (filled-in bars) mice. Quantification of the average frequencies (G) and amplitudes (H) of spontaneous events in *NL2*$^{+/+}$ and *NL2*$^{-/-}$ CA1 neurons.

(I) Representative recordings of GABAergic miniature inhibitory postsynaptic currents (mIPSC) from CA1 pyramidal neurons in acute hippocampal slices from adult *NL2*$^{+/+}$ and *NL2*$^{-/-}$ mice. Quantification of the average frequencies (J) and amplitudes (K) of miniature events in *NL2*$^{+/+}$ and *NL2*$^{-/-}$ CA1 neurons.

(L) Onset kinetics expressed as normalized histograms of rise slopes (peak amplitude in pA over time to onset in milliseconds) of GABAergic mIPSCs in *NL2*$^{+/+}$ and *NL2*$^{-/-}$ neurons. Mean values and the significance of their difference are indicated by squares positioned relative to the x axis of the histogram.

All error bars indicate SEM.

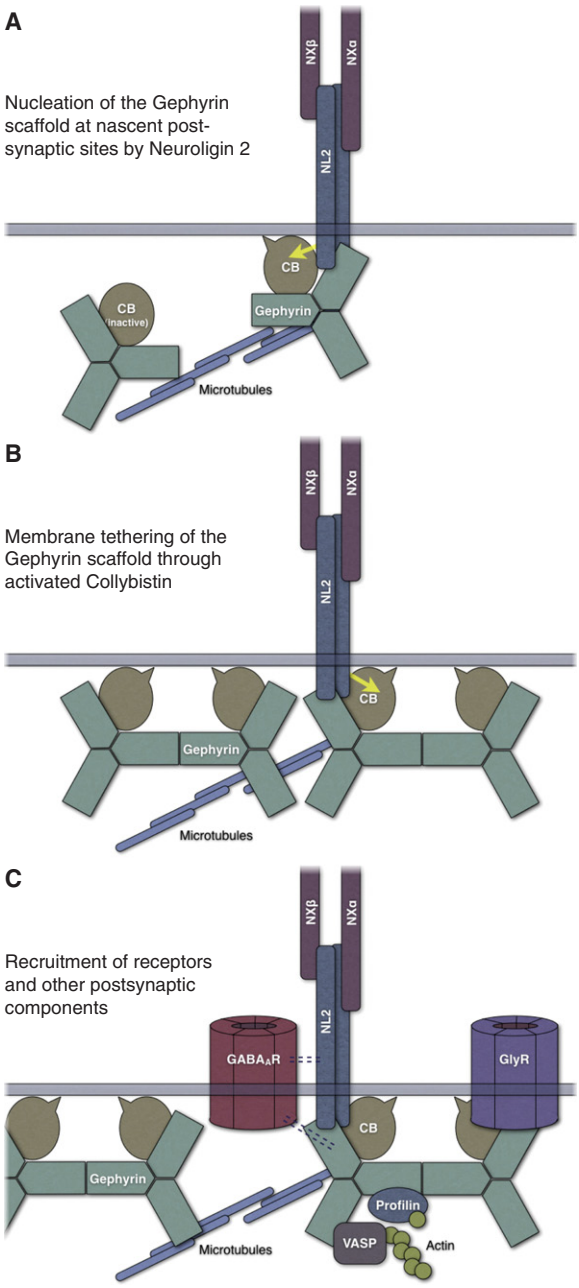

Figure 7. Assembly Model of the Inhibitory Postsynapse

(A) NL2 clusters on the surface of the postsynaptic neuron via *in trans* interactions with α- or β-NXs on contacting inhibitory axon terminals. Cytoplasmic gephyrin-collybistin complexes are transiently recruited to plasma membrane sites of NL2 accumulation via the NL2-gephyrin interaction. Collybistin in complex with gephyrin is activated at these sites by NL2 and the collybistin-gephyrin complex is tethered to the plasma membrane via collybistin.

(B) NL2 clusters further recruit and activate gephyrin-collybistin complexes, acting as nucleation sites for the establishment of a membrane-tethered postsynaptic gephyrin scaffold.

(C) Plasma membrane glycine receptors and other gephyrin-binding proteins are directly recruited to the scaffold. $GABA_A$ receptors are also recruited via potential links to NL2-gephyrin-collybistin complexes. As a result, inhibitory receptors are clustered in precise apposition to presynaptic terminals releasing inhibitory transmitters.

differentially redundant factors. In this context it becomes important to thoroughly examine the potential roles of homologous proteins that could function in the pathway of postsynaptic differentiation proposed here. Other NLs, such as the yet-to-be-studied NL4, might compensate for the loss of NL2 at subsets of inhibitory synapses. Collybistin has numerous homologs that share the same domain organization. Those that would specifically exhibit the properties of collybistin critical for postsynaptic differentiation, namely to interact with gephyrin and membrane lipids and be activated through interaction with NL2 or similar proteins, would be plausible candidates for selective compensation in different brain regions.

In view of the findings reported here, NLs can be considered as core organizers of postsynaptic scaffolds, while NL2 critically functions at perisomatic inhibitory synapses to drive postsynaptic differentiation. These findings provide a mechanistic framework for the further study of the fundamental role of NLs in the establishment of precise and balanced synaptic transmission through their function in postsynaptic assembly of distinct classes of synapses.

EXPERIMENTAL PROCEDURES

Constructs

Epitope-tagged expression constructs of rat myc-NL1 in pcDNA3, HA-NL2 in pcDNA3, and HA-NL3 in pCMV were generously provided by S. Jamain (Göttingen, Germany). An expression construct for human HA-CD8α in pNice vector was generously provided by A.M. Craig (Vancouver, BC, Canada). $GABA_A$ receptor subunit expression constructs α2, β3, and myc-tagged γ2 were generously provided by B. Lüscher (University Park, PA, USA). The FLAG-NX1α expression construct was generously provided by M. Missler (Göttingen, Germany). See Supplemental Experimental Procedures for further constructs.

YTH Screen and Assays

YTH screening was performed against a rat brain cDNA prey library as described previously (Betz et al., 1997) and in the Supplemental Experimental Procedures.

Chemical Crosslinking, Coimmunoprecipitation, and In Vitro Binding Assays

Crosslinking was performed on postnuclear homogenates from a single adult mouse brain in PBS. Homogenates were incubated on ice for 20 min with 200 μM of the cleavable, membrane-permeable crosslinker DSP (Pierce). The crosslinker was quenched in Tris buffer, the material was centrifuged at 21,000 g for 15 min, and proteins were extracted from pellets with 1% SDS in TNE buffer (50 mM Tris, 150 mM NaCl, 5 mM EDTA, 1 μM leupeptin, 1 μg/ml aprotinin, and 100 μM PMSF). Alternatively, crosslinking was performed in situ on live COS7 cells 16 hr posttransfection. Cells were incubated for 20 min on ice with 1 mM DSP in PBS and subsequently lysed as described above. SDS extracts were obtained after centrifugation of either brain or COS7 cell lysates and were diluted with seven volumes of 1% Triton X-100 in TNE to allow for subsequent NL2 IP as described in the Supplemental Experimental Procedures.

In vitro binding assays were performed by GST-pulldown experiments using lysates from *E. coli* BL21 DE3 cells expressing GST- and His-tagged recombinant proteins. Cleared lysates containing GST fusion proteins were incubated with glutathione-Sepharose beads for 2 hr at 4°C and subsequently for 2 hr with cleared lysates of the His-tagged gephyrin E domain in the presence of 1% Triton X-100 in PBS. After washing, bound proteins were eluted at 48°C with buffer containing 25 mM Tris-HCl (pH 7.5), 192 μM glycine, and 0.1% SDS. Eluates were analyzed by SDS-PAGE followed by Coomassie staining to see GST fusion proteins and immunoblotting with mouse anti-His antibody (1:1000, Novagen) to detect His-gephyrin E domain.

Cell Culture and Image Analysis

Culture, transfection, and immunostaining of cell lines were performed as described in the Supplemental Experimental Procedures. All samples within a given set were treated in parallel. Intensity correlation analysis was performed on multichannel images using ImageJ software. Briefly, a Gaussian blur was applied and the HA channel was thresholded. Standard Pearson's correlation coefficient was evaluated between the HA and GFP channels in the thresholded fields using the Intensity Correlation Analysis plugin for ImageJ from T. Collins and E. Stanley (Toronto, ON, Canada).

Hippocampal neurons were prepared from newborn *NL2*$^{-/-}$ mice for transfection experiments or from newborn *NL2*$^{-/-}$ and wild-type littermates for morphological studies (see Supplemental Experimental Procedures). Surface clustering of HA-tagged proteins was achieved after treatment of DIV8 neurons with 5 ng/μl 12CA5 monoclonal IgG_{2b} anti-HA antibody (Roche) for 25 min followed by treatment with 2.5 ng/μl fluorophore-conjugated IgG_{2b} isotype-specific antibody (Molecular Probes) for 25 min at room temperature prior to fixation. Neurons were fixed and immunolabeled for gephyrin and synapsin as described in the Supplemental Experimental Procedures.

To quantify the recruitment of gephyrin at sites of acutely clustered HA-tagged proteins, extrasynaptic HA-immunoreactive surface clusters were designated using standardized intensity thresholding from all transfected neurons identified. As readout for the gephyrin recruitment capacity of HA-tagged proteins, the fluorescence intensity ratio of gephyrin to HA immunoreactivity was measured for each cluster as described in the Supplemental Experimental Procedures.

Morphological analysis of gephyrin distribution was carried out on images acquired using epifluorescence microscopy. Synaptic gephyrin clusters on the somatic plasma membrane were designated by thresholding of gephyrin immunofluorescence and apposition to suprathreshold synapsin immunofluorescence. Cytoplasmic gephyrin aggregates in neurons were distinguished by their characteristic shape, large size, and saturation of fluorescence on acquired images. Gephyrin and synapsin puncta in the neuritic plexus regions of the culture were designated by isodata automated thresholding after high-pass filtering of background fluorescence. Neuritic puncta density was expressed as the ratio of puncta counted over the area of neurite plexus as defined by Otsu automated thresholding after applying a large-kern Gaussian blur to grayscale images combining synapsin and gephyrin immunofluorescence. Quantifications were performed on DIV16 cultured hippocampal neurons.

Preparation, immunolabeling, and imaging of brain sections from adult *NL2*$^{-/-}$, collybistin knockout, and control littermate mice were performed as described in the Supplemental Experimental Procedures.

Electrophysiological Recordings

All electrophysiological and ventilation analyses were performed on P2–P4 mouse pups as described in the Supplemental Experimental Procedures. Briefly, acute slices containing the RVLM and hypoglossal nucleus were used for whole-cell recordings. Spontaneous postsynaptic currents were recorded from neurons of the RVLM at a Cl^- reversal potential of about 0 mV in the presence of 10 μM CNQX and 1 μM strychnine to record GABAergic IPSCs, 10 μM CNQX, and 1 μM bicuculline to record glycinergic IPSCs, and 1 μM bicuculline and strychnine to record glutamatergic EPSCs. Spontaneous miniature GABAergic, glycinergic, and glutamatergic PSCs were recorded as above, but in the presence of 0.5 μM tetrodotoxin. The slope of onset of miniature events was calculated as the change in current amplitude over time of onset in the interval between10% and 90% of peak amplitude. Hippocampal electrophysiological recordings were performed on CA1 pyramidal neurons from acute frontal brain slices from adult mice.

Extracellular pressure ejection of agonists (5 mM muscimol, 5 mM glycine, or 5 mM glutamate in bath solution) was performed in close proximity to the recorded neuron by glass pipettes under constant pressure (0.5 mbar) for 500 ms. The distance between pipette tips and the cell were monitored using an LCD camera and kept constant between recordings.

SUPPLEMENTAL DATA

Supplemental Data include Supplemental Experimental Procedures, eight figures, and one table and can be found with this article online at http://www.cell.com/neuron/supplemental/S0896-6273(09)00635-7.

ACKNOWLEDGMENTS

We are grateful to A.M. Craig (Vancouver, BC, Canada) for her constructive experimental advice. We thank K. Hellmann and A. Galinski (Göttingen) for excellent technical assistance. This work was supported by the Max Planck Society, the German Research Foundation (GRK 521 and FZT 103, F.V. and N.B.), the DFG-Research Center for Molecular Physiology of the Brain (F.V., N.B., and W.Z.), grants from the European Commission (EUSynapse, LSHM-CT-2005-019055; N.B.), (NEUREST, MEST-CT-2004-504193; M.H.), the Cure Autism Now Foundation (F.V.), and the Medical Research Council (G0500833, G0501258 and G0800498; K.H., R.J.H.).

Accepted: August 24, 2009
Published: September 9, 2009

REFERENCES

Betz, A., Okamoto, M., Benseler, F., and Brose, N. (1997). Direct interaction of the rat unc-13 homologue Munc13-1 with the N terminus of syntaxin. J. Biol. Chem. *272*, 2520–2526.

Blundell, J., Tabuchi, K., Bolliger, M.F., Blaiss, C.A., Brose, N., Liu, X., Sudhof, T.C., and Powell, C.M. (2009). Increased anxiety-like behavior in mice lacking the inhibitory synapse cell adhesion molecule neuroligin 2. Genes Brain Behav. *8*, 114–126.

Brose, N. (2009). Synaptogenic proteins and synaptic organizers: many hands make light work. Neuron *61*, 650–652.

Budreck, E.C., and Scheiffele, P. (2007). Neuroligin-3 is a neuronal adhesion protein at GABAergic and glutamatergic synapses. Eur. J. Neurosci. *26*, 1738–1748.

Chih, B., Engelman, H., and Scheiffele, P. (2005). Control of excitatory and inhibitory synapse formation by neuroligins. Science *307*, 1324–1328.

Chih, B., Gollan, L., and Scheiffele, P. (2006). Alternative splicing controls selective trans-synaptic interactions of the neuroligin-neurexin complex. Neuron *51*, 171–178.

Chubykin, A.A., Atasoy, D., Etherton, M.R., Brose, N., Kavalali, E.T., Gibson, J.R., and Sudhof, T.C. (2007). Activity-dependent validation of excitatory versus inhibitory synapses by neuroligin-1 versus neuroligin-2. Neuron *54*, 919–931.

Comoletti, D., Flynn, R., Boucard, A., Demeler, B., Schirf, V., Shi, J., Jennings, L., Newlin, H., Südhof, T., and Taylor, P. (2006). Gene selection, alternative splicing, and post-translational processing regulate neuroligin selectivity for beta-neurexins. Biochemistry *45*, 12816–12827.

Connolly, C.N., Krishek, B.J., McDonald, B.J., Smart, T.G., and Moss, S.J. (1996). Assembly and cell surface expression of heteromeric and homomeric gammaaminobutyric acid type A receptors. J. Biol. Chem. *271*, 89–96.

Craig, A.M., and Kang, Y. (2007). Neurexin-neuroligin signaling in synapse development. Curr. Opin. Neurobiol. *17*, 43–52.

Dean, C., Scholl, F.G., Choih, J., DeMaria, S., Berger, J., Isacoff, E., and Scheiffele, P. (2003). Neurexin mediates the assembly of presynaptic terminals. Nat. Neurosci. *6*, 708–716.

Dong, N., Qi, J., and Chen, G. (2007). Molecular reconstitution of functional GABAergic synapses with expression of neuroligin-2 and GABAA receptors. Mol. Cell. Neurosci. *35*, 14–23.

Essrich, C., Lorez, M., Benson, J.A., Fritschy, J.M., and Luscher, B. (1998). Postsynaptic clustering of major GABAA receptor subtypes requires the gamma 2 subunit and gephyrin. Nat. Neurosci. *1*, 563–571.

Feng, G., Tintrup, H., Kirsch, J., Nichol, M.C., Kuhse, J., Betz, H., and Sanes, J.R. (1998). Dual requirement for gephyrin in glycine receptor clustering and molybdoenzyme activity. Science *282*, 1321–1324.

Fritschy, J.M., Harvey, R.J., and Schwarz, G. (2008). Gephyrin: where do we stand, where do we go? Trends Neurosci. *31*, 257–264.

Graf, E., Zhang, X., Jin, S., Linhoff, M., and Craig, A. (2004). Neurexins induce differentiation of GABA and glutamate postsynaptic specializations via neuroligins. Cell *119*, 1013–1026.

Harvey, K., Duguid, I.C., Alldred, M.J., Beatty, S.E., Ward, H., Keep, N.H., Lingenfelter, S.E., Pearce, B.R., Lundgren, J., Owen, M.J., et al. (2004). The GDPGTP exchange factor collybistin: an essential determinant of neuronal gephyrin clustering. J. Neurosci. *24*, 5816–5826.

Hirao, K., Hata, Y., Ide, N., Takeuchi, M., Irie, M., Yao, I., Deguchi, M., Toyoda, A., Sudhof, T.C., and Takai, Y. (1998). A novel multiple PDZ domain-containing molecule interacting with N-methyl-D-aspartate receptors and neuronal cell adhesion proteins. J. Biol. Chem. *273*, 21105–21110.

Hoon, M., Bauer, G., Fritschy, J.M., Moser, T., Falkenburger, B.H., and Varoqueaux, F. (2009). Neuroligin 2 controls the maturation of GABAergic synapses and information processing in the retina. J. Neurosci. *29*, 8039–8050.

Ichtchenko, K., Hata, Y., Nguyen, T., Ullrich, B., Missler, M., Moomaw, C., and Südhof, T. (1995). Neuroligin 1: a splice site-specific ligand for beta-neurexins. Cell *81*, 435–443.

Ichtchenko, K., Nguyen, T., and Südhof, T. (1996). Structures, alternative splicing, and neurexin binding of multiple neuroligins. J. Biol. Chem. *271*, 2676–2682.

Irie, M., Hata, Y., Takeuchi, M., Ichtchenko, K., Toyoda, A., Hirao, K., Takai, Y., Rosahl, T.W., and Sudhof, T.C. (1997). Binding of neuroligins to PSD-95. Science *277*, 1511–1515.

Jamain, S., Radyushkin, K., Hammerschmidt, K., Granon, S., Boretius, S., Varoqueaux, F., Ramanantsoa, N., Gallego, J., Ronnenberg, A., Winter, D., et al. (2008). Reduced social interaction and ultrasonic communication in a mouse model of monogenic heritable autism. Proc. Natl. Acad. Sci. USA *105*, 1710–1715.

Kalscheuer, V.M., Musante, L., Fang, C., Hoffmann, K., Fuchs, C., Carta, E., Deas, E., Venkateswarlu, K., Menzel, C., Ullmann, R., et al. (2009). A balanced chromosomal translocation disrupting ARHGEF9 is associated with epilepsy, anxiety, aggression, and mental retardation. Hum. Mutat. *30*, 61–68.

Kang, Y., Zhang, X., Dobie, F., Wu, H., and Craig, A.M. (2008). Induction of GABAergic postsynaptic differentiation by alpha-neurexins. J. Biol. Chem. *283*, 2323–2334.

Kim, E., and Sheng, M. (2004). PDZ domain proteins of synapses. Nat. Rev. Neurosci. *5*, 771–781.

Kins, S., Betz, H., and Kirsch, J. (2000). Collybistin, a newly identified brain-specific GEF, induces submembrane clustering of gephyrin. Nat. Neurosci. *3*, 22–29.

Kirsch, J., Wolters, I., Triller, A., and Betz, H. (1993). Gephyrin antisense oligonucleotides prevent glycine receptor clustering in spinal neurons. Nature *366*, 745–748.

Kneussel, M., Brandstatter, J.H., Laube, B., Stahl, S., Muller, U., and Betz, H. (1999). Loss of postsynaptic GABA(A) receptor clustering in gephyrin-deficient mice. J. Neurosci. *19*, 9289–9297.

Kneussel, M., Engelkamp, D., and Betz, H. (2001). Distribution of transcripts for the brain-specific GDP/GTP exchange factor collybistin in the developing mouse brain. Eur. J. Neurosci. *13*, 487–492.

Leonard, A.S., Davare, M.A., Horne, M.C., Garner, C.C., and Hell, J.W. (1998). SAP97 is associated with the alpha-amino-3-hydroxy-5-methylisoxazole-4-propionic acid receptor GluR1 subunit. J. Biol. Chem. *273*, 19518–19524.

Levinson, J.N., Chery, N., Huang, K., Wong, T.P., Gerrow, K., Kang, R., Prange, O., Wang, Y.T., and El-Husseini, A. (2005). Neuroligins mediate excitatory and inhibitory synapse formation: involvement of PSD-95 and neurexin-1beta in neuroligin-induced synaptic specificity. J. Biol. Chem. *280*, 17312–17319.

Linhoff, M.W., Lauren, J., Cassidy, R.M., Dobie, F.A., Takahashi, H., Nygaard, H.B., Airaksinen, M.S., Strittmatter, S.M., and Craig, A.M. (2009). An unbiased expression screen for synaptogenic proteins identifies the LRRTM protein family as synaptic organizers. Neuron *61*, 734–749.

Löw, K., Crestani, F., Keist, R., Benke, D., Brunig, I., Benson, J.A., Fritschy, J.M., Rulicke, T., Bluethmann, H., Mohler, H., and Rudolph, U. (2000). Molecular and neuronal substrate for the selective attenuation of anxiety. Science *290*, 131–134.

Meyer, G., Kirsch, J., Betz, H., and Langosch, D. (1995). Identification of a gephyrin binding motif on the glycine receptor beta subunit. Neuron *15*, 563–572.

Meyer, G., Varoqueaux, F., Neeb, A., Oschlies, M., and Brose, N. (2004). The complexity of PDZ domain-mediated interactions at glutamatergic synapses: a case study on neuroligin. Neuropharmacology *47*, 724–733.

Miles, R., Toth, K., Gulyas, A.I., Hajos, N., and Freund, T.F. (1996). Differences between somatic and dendritic inhibition in the hippocampus. Neuron *16*, 815–823.

Moss, S., and Smart, T. (2001). Constructing inhibitory synapses. Nat. Rev. Neurosci. *2*, 240–250.

Nusser, Z., Sieghart, W., Benke, D., Fritschy, J.M., and Somogyi, P. (1996). Differential synaptic localization of two major gamma-aminobutyric acid type A receptor alpha subunits on hippocampal pyramidal cells. Proc. Natl. Acad. Sci. USA *93*, 11939–11944.

Papadopoulos, T., Korte, M., Eulenburg, V., Kubota, H., Retiounskaia, M., Harvey, R.J., Harvey, K., O'Sullivan, G.A., Laube, B., Hulsmann, S., et al. (2007). Impaired GABAergic transmission and altered hippocampal synaptic plasticity in collybistindeficient mice. EMBO J. *26*, 3888–3899.

Papadopoulos, T., Eulenburg, V., Reddy-Alla, S., Mansuy, I.M., and Betz, H. (2008). Collybistin is required for both the formation and maintenance of GABAergic postsynapses in the hippocampus. Mol. Cell. Neurosci. *39*, 161–169.

Prior, P., Schmitt, B., Grenningloh, G., Pribilla, I., Multhaup, G., Beyreuther, K., Maulet, Y., Werner, P., Langosch, D., and Kirsch, J. (1992). Primary structure and alternative splice variants of gephyrin, a putative glycine receptor-tubulin linker protein. Neuron *8*, 1161–1170.

Richter, D.W., and Spyer, K.M. (2001). Studying rhythmogenesis of breathing: comparison of in vivo and in vitro models. Trends Neurosci. *24*, 464–472.

Scheiffele, P., Fan, J., Choih, J., Fetter, R., and Serafini, T. (2000). Neuroligin expressed in nonneuronal cells triggers presynaptic development in contacting axons. Cell *101*, 657–669.

Sola, M., Bavro, V.N., Timmins, J., Franz, T., Ricard-Blum, S., Schoehn, G., Ruigrok, R.W., Paarmann, I., Saiyed, T., O'Sullivan, G.A., et al. (2004). Structural basis of dynamic glycine receptor clustering by gephyrin. EMBO J. *23*, 2510–2519.

Song, J., Ichtchenko, K., Südhof, T., and Brose, N. (1999). Neuroligin 1 is a postsynaptic cell-adhesion molecule of excitatory synapses. Proc. Natl. Acad. Sci. USA *96*, 1100–1105.

Tretter, V., Jacob, T.C., Mukherjee, J., Fritschy, J.M., Pangalos, M.N., and Moss, S.J. (2008). The clustering of GABA(A) receptor subtypes at inhibitory synapses is facilitated via the direct binding of receptor alpha 2 subunits to gephyrin. J. Neurosci. *28*, 1356–1365.

Ullrich, B., Ushkaryov, Y.A., and Sudhof, T.C. (1995). Cartography of neurexins: more than 1000 isoforms generated by alternative splicing and expressed in distinct subsets of neurons. Neuron *14*, 497–507.

Ushkaryov, Y.A., Hata, Y., Ichtchenko, K., Moomaw, C., Afendis, S., Slaughter, C.A., and Sudhof, T.C. (1994). Conserved domain structure of beta-neurexins. Unusual cleaved signal sequences in receptor-like neuronal cell-surface proteins. J. Biol. Chem. *269*, 11987–11992.

Ushkaryov, Y.A., Petrenko, A.G., Geppert, M., and Sudhof, T.C. (1992). Neurexins: synaptic cell surface proteins related to the alpha-latrotoxin receptor and laminin. Science *257*, 50–56.

Varoqueaux, F., Jamain, S., and Brose, N. (2004). Neuroligin 2 is exclusively localized to inhibitory synapses. Eur. J. Cell Biol. *83*, 449–456.

Varoqueaux, F., Aramuni, G., Rawson, R., Mohrmann, R., Missler, M., Gottmann, K., Zhang, W., Südhof, T., and Brose, N. (2006). Neuroligins determine synapse maturation and function. Neuron *51*, 741–754.

Yamagata, M., Sanes, J.R., and Weiner, J.A. (2003). Synaptic adhesion molecules. Curr. Opin. Cell Biol. *15*, 621–632.